J Mater Sci (2007) 42:8029–8034
DOI 10.1007/s10853-006-1485-6

POLYMER FIBERS 2006

Electrospinning of chitosan nanofibrous structures: feasibility study

Sander De Vrieze · Philippe Westbroek · Tamara Van Camp · Lieva Van Langenhove

Received: 4 September 2006 / Accepted: 26 December 2006 / Published online: 15 May 2007

Abstract In this paper a range of acid aqueous solutions are studied towards their suitability for developing chitosan nanofibres by electrospinning. It was found that parameters such as type of solvent, pH, concentration of chitosan, viscosity, charge density, applied voltage, solution flow rate, distance from nozzle tip to collector surface and time play a role in the characteristics of the obtained nanofibrous structures. After a preliminary study to select the most suitable composition of the chitosan containing solution (90% acetic acid), a detailed study was done to find the optimal conditions for chitosan nanofibrous structure development. Finally long-term experiments were performed, which showed that the formation of the nanofibrous structure distorts the electrical field.

Introduction

Electrospinning is a powerful method for the fabrication of (nano)fibrous structures and various polymers have been electrospun into ultrafine fibers with diameters in the area of 20–400 nm [1–24]. Application of an electrical field between a needle and a collector surface (metallic plate) causes a deformation of the polymer fluid from a spherical pendant drop to a conical shape (Taylor cone). At a certain value, this electrical field surpasses the threshold value where the electrostatic repulsion force of charges located at the surface of the drop overcome surface tension. This results in the ejection of a charged fluid jet from the tip of the Taylor cone and transported towards the collector. On its way the jet becomes unstable, due to interaction of the charges with the external electrical field and solvent evaporation, which causes bending and splaying. This results in the deposition of ultrafine and long (order of meter) nanofibres as a non-woven structure.

Besides charge density and applied voltage also other parameters influence the final nanofibrous structure and its properties, for example: polymer type and concentration, type of solvent, presence of electrolyte, type and concentration of electrolyte, viscosity, surface tension, tip-to-collector distance, flow rate of the polymer solution, inner diameter of the tip, material of the tip, etc.

The obtained nanofibrous structures have interesting characteristics such as large specific surface area (e.g. 1 g of polymer results in about 100 m^2 when nanofibre diameter is 50 nm), high porosity, high absorbance capacity and a very flat surface (roughness is determined at nanolevel). Therefore nanofibrous structures are promising materials for applications in medical sector (tissue engineering, wound dressing, drug delivery), hygiene industry (napkins, wipers, absorbers), filter industry (nanofiltration, exchange membranes, ab- and adsorption systems), intelligent textiles (sensing, actuating) and for coatings (multifunctional coatings).

Chitosan is a biodegradable polymer obtained from a deacetylation reaction of chitin [25, 26]. Chitosan showed promising characteristics towards improved burn wound healing and in environmental applications for the removal of heavy metals, such as cadmium, chromium, copper, lead and mercury by coordination between the metals and the amine groups present at the chitosan structure. The impact of these characteristics can be improved by increasing the

S. De Vrieze · P. Westbroek (✉) · T. Van Camp · L. Van Langenhove
Department of Textiles, Ghent University, Technologiepark 907, 9052 Gent, Belgium
e-mail: Philippe.westbroek@Ugent.be

specific surface area for which the development of nanofibrous structures of chitosan would be an excellent possibility.

Chitosan has been electrospun before mainly from polymer mixtures of chitosan and polyethylene oxide (PEO) [27–29] and chitosan with polyvinylalcohol (PVA) [30, 31]. Also pure chitosan fibers were obtained in strong acetic acid [32] and strong trifluoroacetic acid [33] solutions.

In this paper it is the aim to obtain pure chitosan fibrous structures, which can be useful for applications in medical sector, mainly for wound treatment and in environmental applications for the removal of metals from solution.

Experimental

Chitosan (1.9–3.1 $\times$ 10^5 g mol^{-1}, degree of de-acetylation is 75–85%); formic acid, acetic acid, lactic acid and hydrochloric acid were obtained from Sigma-Aldrich. Deionised water was used throughout the investigation obtained by treatment of domestic water in an ion-exchanger Millipore-Q-system.

The setup for electrospinning is represented in Fig. 1. With a high voltage DC (direct current) source a potential difference of a few kV cm^{-1} is applied between two metallic plates. Polymer solution was pumped from a syringe (Sigma-Aldrich) with luer-lock connections to the tip of a metallic capillary using an anesthesia pump type KDS series 100. The polymer jet is formed from a Taylor cone and transforms into nanofibrous structures on its way to the collector, while solvent is evaporating. This results in the deposition of a non-woven nanofibrous structure.

Preliminary analysis of the nanofibrous structures was done with an Olympus BX51 microscope on which a Sony 3CCD color video camera, type DXC-930P is connected. For picture treatment and analysis a Lucia 4.51 software package was used. This instrument was only used for a rough picture of the nanofibrous structures. Detailed pictures were obtained with SEM (FEI Quanta 200 F) as well as the determination of the nanofibre diameters, for which the resolution of the Olympus microscope was not high enough.

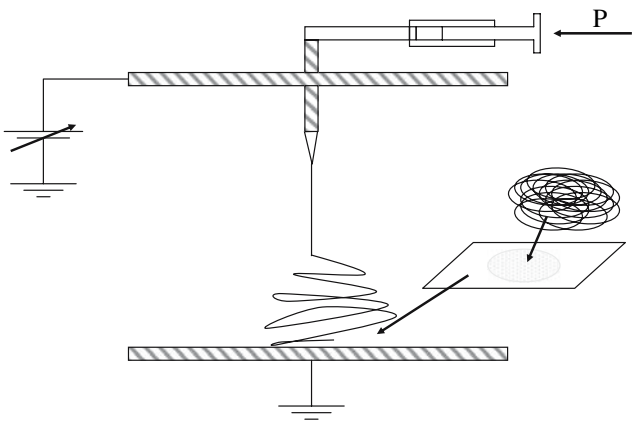

Fig. 1 Principle scheme of the electrospinning setup

Results and discussion

Preliminary study towards electrospinnability of chitosan solutions

Chitosan is known to dissolve in acidic aqueous solutions due to the amine functions present in the chemical structure. Therefore a range of solutions was prepared (Table 1) and used in the electrospinning equipment. For this preliminary study 3 parameters were varied, for each parameter focus was given to 3 values (Table 2) and all possible combinations of parameter values were investigated. This means that for each solution 27 experiments were performed. Analysis of the results was done by visual detection during the experiment and by microscopic pictures taken of the resulting deposition at the collector surface. A set of requirements were defined to rate the success of electrospinnability of the solution. For success all of the following requirements need to be fulfilled:

- formation of a Taylor cone at the tip of the nozzle (visual detection)
- formation of a stable jet (visual detection)
- uniform distribution of the deposited fibres at macroscale (visual detection)
- formation of fibres with diameters less than 500 nm (microscopic and SEM detection)

The formation of a Taylor cone at the tip of the nozzle is strongly dependent on the viscosity of the solution. First all proposed solvents and acidic solutions were electrospun in the absence of dissolved chitosan and did not result in the formation of a Taylor cone, as was expected based on their limited viscosity. Dissolving chitosan increases the viscosity. For solutions 4–12 a well defined Taylor cone was observed, while for solutions 1–3 a similar behaviour was obtained as observed with solutions not containing chitosan. The relatively small concentration of chitosan (<2%) that can be dissolved in these solutions can explain this effect, but this is not the only reason. As can be seen in Table 1 also solutions 6 and 7 contain only 2% of chitosan. The difference with solutions 1–3 is that the pH of solutions 6 and 7 is much lower (strong acidic solutions). This includes that the fraction of amine functions that is protonated is much higher in solutions 6 and 7 compared to

Table 1 Composition of the solutions analysed for electrospinnability using electrospinning parameters of Table 2

Sol Nr.	Conc. CH_3COOH (m%)	Conc. HCl (m%)	Conc. $CH_3CH(OH)COOH$ (m%)	Conc. HCOOH (m%)	Max. conc. Chitosan (m%)	Electro-spinnability
1	2	–	–	–	2	Negative
2	5	1	5	–	2	Negative
3	5	–	5	–	1	Negative
4	–	–	–	100	3	Negative
5	–	–	–	90	4	Negative
6	–	–	85	–	2	Negative
7	10	–	75	–	2	Negative
8	15	–	70	–	3	Negative
9	60	–	30	–	4	Negative
10	90	–	–	–	5	Positive
11	85	–	–	–	5	Positive
12	80	–	–	–	4	Positive

solutions 1–3. It also increases the charged state of the chitosan polymer chain. The charge density has an effect on the electrospinnability since a high voltage difference between nozzle and collector surface is applied. This explains why for solutions 6 and 7 a Taylor cone is obtained and not for solutions 1–3, although equal concentrations of chitosan were used.

Although that for solutions 4–12 a Taylor cone was observed, the other criteria for success were not fulfilled for solutions 4–9. For none of these solutions a stable jet was obtained. After formation of the Taylor cone and a jet of solution between the tip of the nozzle and the collector surface it is stable for a few seconds followed by an explosion of the cone and the jet, resulting in the deposition of solution drops surrounded by a sort of fibre like structure. Microscopic pictures showed clearly the formation of drops and not fibres, definitely not nanofibres. It is believed that the concentration of the chitosan polymer is still too small. Although the concentrations are high enough to obtain a suitable viscosity, it is too small to initiate a high degree of entanglement during solvent evaporation in the jet. This entanglement is needed for fibre formation and locally the charge density increases seriously because of solvent evaporation. This causes inhomogeneous charge distributions over the jet, which explains the ''explosion''. A higher concentration of chitosan would result in a large degree of entanglement and formation of strong pre-fibrous structures that overcome the repulsive forces caused by inhomogeneous charge distributions.

Solutions 10–12 resulted in successful experiments. The following parameters were investigated: applied potential, distance between tip of the nozzle and the collector surface and flow rate of the solution (Table 2). It was found that a well defined Taylor cone was formed, a stable jet was obtained and a uniform white deposition was observed at the collector surface. SEM pictures showed interesting nanofibrous structures with nanofibres having diameters in the range of 50–100 nm. An example is given in Fig. 2, which was taken from a 3% chitosan in 90% acetic acid solution at 20 kV applied over a distance of 10 cm and a flow rate of 1 mL h^{-1}. Well-defined nanofibres are observed except from a few beads, which is quite normal since it is a preliminary experiment. The success rate for

Table 2 Values for the electrospinning parameters used in the preliminary study towards electrospinnability of the solutions given in Table 1

Applied voltage (kV)	10	20	30
Distance nozzle to collector (cm)	10	15	20
Solution flow rate (mL h^{-1})	1	5	10

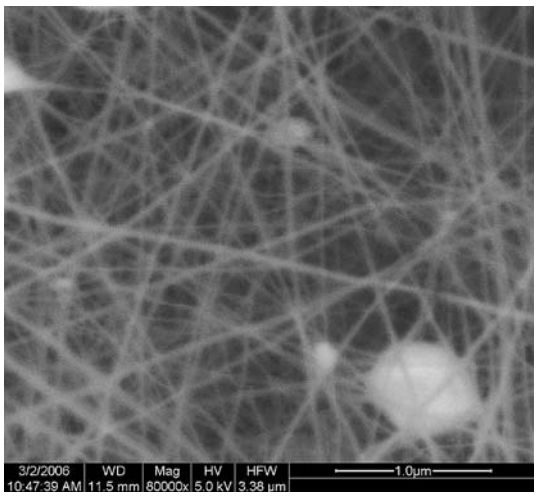

Fig. 2 SEM picture taken from a 3% chitosan in 90% acetic acid solution (solution number 10) at 20 kV applied over a nozzle to collector distance of 10 cm and a solution flow rate of 1 mL h^{-1}

obtaining nanofibres in strongly concentrated acetic acid solutions is based on the relatively higher concentrations of chitosan (about 5%) that can be obtained. Such concentrations result in an optimal viscosity for electrospinning, but also contribute to the degree of entanglement of polymer chains in the jet. The latter results in the formation of fibres instead of the ''explosion'' of the jet and the Taylor cone. The solution is strongly acidic, thus the polymers are well aligned in the electrical field because of the high fraction of protonated (thus charged) amine functions. This also promotes entanglement of the polymer chains.

Detailed study of the nanofibres obtained from chitosan-strong acetic acid solutions

In this section it is the aim to find the optimal conditions of the processing parameters, given in Table 3, for the deposition of chitosan nanofibres. Important observations that will determine the selection of the optimal values are uniformity of the deposition at nanolevel, diameter of the fibres, distribution of the fibre thickness and absence of bead formation.

It was observed visually that for chitosan concentrations below 2% the requirements for electrospinnability were not fulfilled, for concentrations above 4% the viscosity of the solution was too high, which resulted in an unstable jet. Further research on solutions containing between 2 and 4% chitosan revealed that 3% (Table 4) is the optimal value. Analysis of the SEM pictures (not shown to avoid overloading of the paper with too many SEM pictures) learned that for 3% chitosan solutions the thinnest nanofibres were obtained with the smallest distribution of nanofibre diameter (70±45 nm, Fig. 3).

No remarkable differences were observed in nanofibre properties as a function of concentration of acetic acid. The 90% solutions have a somewhat smaller diameter compared to the other acetic acid concentrations, therefore 90% is selected as the optimal value (Table 4). Also the distribution of the diameter was observed to be smaller for this concentration.

The optimal applied voltage was observed around 20 kV for a distance of 10 cm (Table 4). For smaller or higher distances from nozzle to collector also a lower or higher optimal applied voltage value was obtained. Normalization of these values learned that a constant value was obtained for the applied voltage per unit of length, being 2.0 kV cm^{-1}.

Finally, the solution flow rate was found to be optimal at 0.3 mL h^{-1} (Table 4). Below this value the transport of solution towards the tip of the nozzle is too small, resulting in unstable Taylor cones and jets, while for higher flow rates thick fibres were obtained.

Table 3 Variation of the processing parameters for electrospinning of chitosan nanofibres from strong acetic acid solutions

Parameter	Dynamic window
Concentration of chitosan (m%)	1–5
Concentration of acetic acid (m%)	80–90
Nozzle to collector distance (cm)	5–20
Solution flow rate (mL h^{-1})	0.1–3
Applied voltage (kV)	5–30

Table 4 Optimal values for the electrospinning of chitosan nanofibrous structures from a strong acetic acid solution

Parameter	Optimal value for electrospinning of chitosan
Concentration of chitosan (m%)	3.0
Concentration of acetic acid (m%)	90
Nozzle to collector distance (cm)	10
Solution flow rate (mL h^{-1})	0.3
Applied voltage (kV)	20
Optimal voltage per length unit (kV cm^{-1})	2.0

Long-term stability of the electrospinning jet and time effects on the chitosan fibres

Long-term stability experiments were performed under optimal conditions as defined in Table 4. It was found that the jet of the chitosan solution remained stable for a couple of hours, after that it became unstable and was distorted towards the edges of the collector surface. SEM pictures were taken after 4 (Fig. 3), 12 (Fig. 4a), 20 (Fig. 4b) and

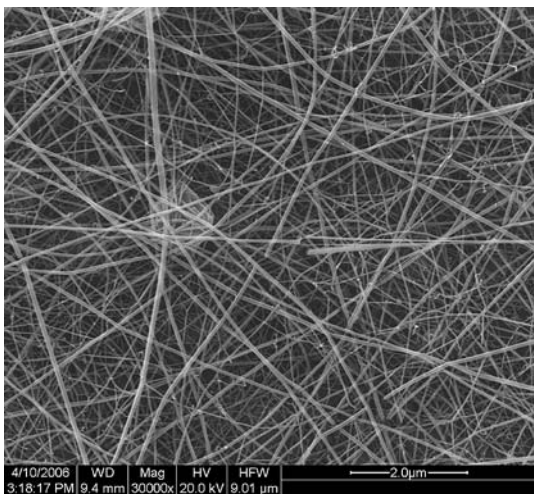

Fig. 3 SEM picture taken from a 3% chitosan in 90% acetic acid solution at 20 kV applied over a nozzle to collector distance of 10 cm and a solution flow rate of 0.3 mL h^{-1}. Deposition time is 4 min

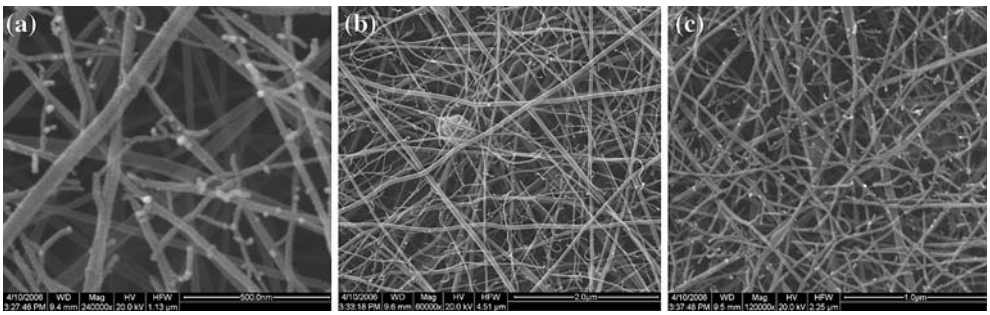

Fig. 4 SEM picture taken from a 3% chitosan in 90% acetic acid solution at 20 kV applied voltage over a nozzle to collector distance of 10 cm and a solution flow rate of 0.3 mL h^{-1}. Deposition time is (**a**) 12; (**b**) 20 and (**c**) 30 min

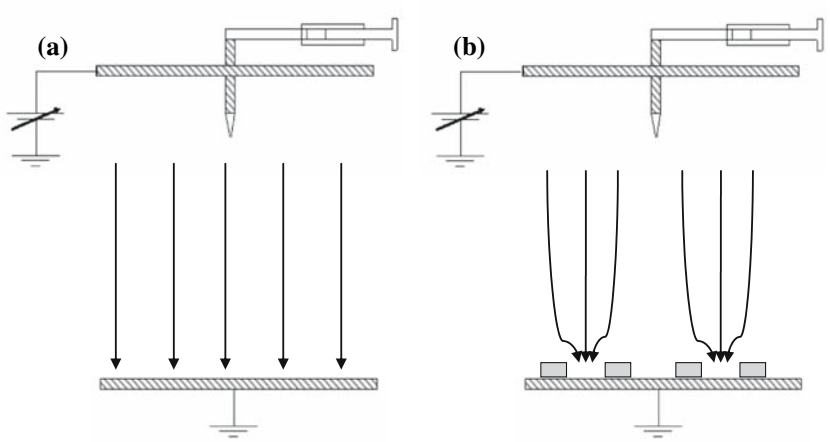

Fig. 5 Schematic drawing of the electrospinning setup and the electrical field lines at (**a**) the initial phase of fibre production and (**b**) after that nanofibres are deposited at the collector surface

30 min (Fig. 4c) of fibre production. After 4 min well-defined nanofibres are obtained without beads or irregularities. However, for longer production time it seems that the nanofibres split and form short side arms on the main fibre. This can be explained by distortion of the electrical field during fibre deposition. At the start of the experiment the electrical field distribution between nozzle and collector surface is homogeneous (Fig. 5a). After some time of fibre deposition the field is distorted in the vicinity of the deposited nanofibrous structure (in its pores) because this structure behaves as an isolator that is brought into the system between nozzle and collector (Fig. 5b). As explained before, inhomogeneous charge distributions are obtained in the jet due to solvent evaporation and for very high applied voltages, which can lead to splitting of the jet. In fact, this is what happens in the pores of the nanofibrous structure. In the vicinity of the pore of the deposited nanofibrous structure the electrical fields are enhanced intensively. Therefore repulsion, due to inhomogeneous charge distribution in the jet and the pre-fibre will become more important and results in splitting of the jet. Since the distance between the point of jet splitting and collector is small the side arms obtained are also short.

The instability of the jet after some hours can be explained in the same way. During electrospinning more and more chitosan fibres are deposited, thus an isolator is building up at the collector surface. This isolation becomes so intensive after some hours that the electrical field lines are distorted towards the edge of the collector (which is still free of nanofibres) and thus the jet is aligned along these field lines.

Conclusion

Chitosan nanofibres with a diameter of about 70 ± 45 nm were obtained from a strong acidic acetic acid solution (90%) with a 3% chitosan concentration at an applied voltage of 2.0 kV cm^{-1} and a flow rate of 0.3 mL h^{-1}. The latter already indicates that possible applications will fall in the field of high performance applications because of slow production time. The formation of nanofibrous structures over longer periods also showed that a time effect is important.

References

1. Hong KH, Oh KW, Kang TJ (2002) J Appl Polym Sci 96:983
2. Shin CY, Chase GG (2005) Polym Bull 55:209
3. Jeun JP, Lim YM, Nho YC (2005) J Ind Eng Chem 11:573
4. Lee HK, Jeong EH, Baek CK, Youk JH (2005) Mater Lett 59:2977

5. Bellan LM, Kameoka J, Craighead HG (2005) Nanotechnol 16:1095
6. Wen XT, Fan HS, Tan YF, Cao HD, Li H, Cai B, Zhang XD (2005) Adv Biomater Key Eng Mater 288–289:139
7. Kim B, Park H, Lee SH, Sigmund WM (2005) Mater Lett 59:829
8. Jun Z, Hou HQ, Wendorff JH, Greiner A (2005) E-Polym art. no. 038
9. Chung GS, Jo SM, Kim BC (2005) J Appl Polym Sci 97:165
10. Riboldi SA, Sampaolesi M, Neuenschwander P, Cossu G, Mantero S (2005) Biomater 26:4606
11. Cha DI, Kim HY, Lee KH, Jung YC, Cho JW, Chun BC (2005) J Appl Polym Sci 96:460
12. Buttafoco L, Kolkman NG, Poot AA, Dijkstra PJ, Vermes I, Feijen J (2005) J Control Drug Release 101:322
13. Han SO, Son WK, Youk JH, Lee TS, Park WH (2005) Mater Lett 59:2998
14. Kim CW, Frey MW, Marquez M, Joo YL (2005) J Polym Sci B—Polym Phys 43:1673
15. Khil MS, Kim HY, Kang YS, Bang HJ, Lee DR, Doo JK (2005) Macromol Res 13:62
16. Subramanian A, Vu D, Larsen GF, Lin HY (2005) J Biomater Sci—Polym Ed 16:861
17. Pornsopone V, Supaphol P, Rangkupan R, Tantayanon S (2005) Polym Eng Sci 45:1073
18. Gupta P, Elkins C, Long TE, Wilkes GL (2005) Polymer 46:4799
19. Kim SH, Nair S, Moore E (2005) Macromol 38:3719
20. Stephens JS, Fahnestock SR, Farmer RS, Kiick KL, Chase DB, Rabolt JF (2005) Biomacromol 6:1405
21. Ayutsede J, Gandhi M, Sukigara S, Micklus M, Chen HE, Ko F (2005) Polym 46:1625
22. Guan HY, Shao CL, Liu YC, Han DX, Yang XH, Yu N (2004) Chem J Chin Univ 25:1413
23. Dharmaraj N, Park HC, Kim CK, Kim HY, Lee DR (2004) Mater Chem Phys 87:5
24. Ding B, Kim CK, Kim HY, Se MK, Park SJ (2004) Fibers Polym 5:105
25. Van De Velde K, Kiekens P (2004) Carbohydrate Polym 58:409
26. Kumar MNVR (2000) Reactive Functional Polym 46:1
27. Duan B, Dong C, Yuan X, Yao K (2004) J Biomater Sci Polym Ed 15:797
28. Spasova M, Manolova N, Paneva D, Rashkov I (2004) E-Polym 56:1
29. Bhattarai N, Edmondson D, Veiseh O, Matsen F, Zhanq M (2005) Biomater 26:6176
30. Martinova L, Mullerova J (2005) 5th World Textile Conference AUTEX, 624–628
31. Li L, Hsieh Y-L (2006) Carbohydrate Res 341:374–381
32. Geng X, Kwon OH, Jang J (2005) Biomater 26:5427–5432
33. Ohkawa K, Cha D, Kim H, Nishida A, Yamamoto H (2004) Macromol Rap Commun 25:1600–1605